Complete one-loop calculation of electroweak supersymmetric effects in t-channel single top production at CERN LHC

M. Beccaria,[1,2] C. M. Carloni Calame,[3] G. Macorini,[4,5] E. Mirabella,[6] F. Piccinini,[7] F. M. Renard,[8] and C. Verzegnassi[4,5]

[1]*Dipartimento di Fisica, Università del Salento, Via Arnesano, I-73100 Lecce, Italy*
[2]*INFN, Sezione di Lecce, Italy*
[3]*INFN, Italy and School of Physics & Astronomy, University of Southampton, Southampton S017 1BJ, England*
[4]*Dipartimento di Fisica Teorica, Università di Trieste, Strada Costiera 14, Miramare (Trieste), Italy*
[5]*INFN, Sezione di Trieste*
[6]*Max-Planck-Institut für Physik, Föhringer Ring 6 D-80805 München, Germany*
[7]*INFN, Sezione di Pavia, Via A. Bassi 6, I-27100 Pavia, Italy*
[8]*Laboratoire de Physique Théorique et Astroparticules, UMR 5207, Université Montpellier II, F-34095 Montpellier Cedex 5.*

(Received 13 February 2008; revised manuscript received 29 April 2008; published 27 June 2008)

We have computed the complete one-loop electroweak effects in the minimal supersymmetric standard model for single top (and single antitop) production in the t channel at hadron colliders, generalizing a previous analysis performed for the dominant dt final state and fully including QED effects. The results are quite similar for all processes. The overall standard model one-loop effect is small, of the few percent size. This is due to a compensation of weak and QED contributions that are of opposite sign. The genuine supersymmetry contribution is generally quite modest in the minimal supergravity scenario. The experimental observables would therefore only practically depend, in this framework, on the Cabibbo-Kobayashi-Maskawa Wtb coupling.

DOI: 10.1103/PhysRevD.77.113018 PACS numbers: 12.15.−y, 12.15.Lk, 13.75.Cs, 14.80.Ly

I. INTRODUCTION

The relevance of a precise measurement of single top production at hadron colliders was already stressed in several papers in the recent years [1]. A well-known peculiarity of the process is actually the fact that it offers the unique possibility of a direct measurement of the Wtb coupling V_{tb}, thus allowing severe tests of the conventionally assumed properties of the Cabibbo-Kobayashi-Maskawa (CKM) matrix in the minimal standard model (SM); for a very accurate review of the topics we defer to [2].

For the specific purpose of a ''precise'' determination of V_{tb}, two independent requests must be met. The first one is that of a correspondingly precise experimental measurement of the process. For the t-channel case on which we shall concentrate on in this paper the CMS study [3] concludes that with 10 fb^{-1} of integrated luminosity, one could be able to reduce the (mostly systematic) experimental uncertainty of the cross section below the 10% level (worse uncertainties are expected for the two other processes, the s channel and the associated Wt production, whose cross section is definitely smaller than that of the t channel). The second request is that of a similarly accurate theoretical prediction of the observables of the process. In this respect, one must make the precise statement that in order to cope with the goal of measuring V_{tb} at the few (5) percent level, a complete next-to-leading order (NLO) calculation is requested. In the SM this has been done for the QCD component of the t channel, resulting in a relatively small (few percent) effect [4]. The electroweak effects have been computed very recently at the complete one-loop level within the Minimal Supersymmetric Standard Model (MSSM) for the dominant $ub \to dt$ component of the process (to be defined in Sec. II) [5].

One conclusion was that the genuine supersymmetry (SUSY) effect, for a set on minimal supergravity (mSUGRA) benchmark points, was systematically modest, roughly at the 1–2% level. The SM contribution was computed in a preliminary way, i.e. only including the soft photon radiation to achieve cancellation of infrared singularities, ignoring the potentially relevant hard photon contribution. Actually, the main purpose of [5] was that of investigating the possible existence and size of genuine supersymmetric effects, that would be essentially unaffected by the SM QED contribution. In this approximate approach, the one-loop SM contribution turned out to be sizable, of roughly 10% on the total rate. This contribution should be considered as a perfectly known term, to be included in the theoretical expression of the rate and compared with the corresponding experimental measurement to extract the precise value of the Wtb coupling V_{tb}.

In fact, from the negative (for what concerns supersymmetric searches) result that the t-channel rate is not sensitive to genuine mSUGRA MSSM effects, adding the extra-known feature that NLO QCD effects are small, of the order of 5%, and well under control [6–8], one concludes that an extremely precise theoretical determination of the process would be possible, provided that a rigorous electroweak one-loop description were given. This requires two different steps: first, an extension of the calculation

 © 2008 The American Physical Society

of [5] to the seven remaining t-channel processes, since the final dt state is only the numerically dominant one. Second, the additional calculation of the complete QED effect, including properly hard photon radiation. This is precisely the aim of this paper, whose goal will be that of offering a clean theoretical expression to be used for a significant measurement of V_{tb}. Technically speaking, this paper is organized as follows. In Sec. II, the definition of the eight considered processes will be given, and the main tasks that were fulfilled to perform a complete one-loop electroweak calculation will be indicated. Since the problems to be solved were practically identical with those already met in d, our description will be whenever possible quick and essential. In Sec. III, we shall expose the new calculation of the complete QED effects. In Sec. IV, we briefly discuss the one-loop SUSY QCD effects that we have recomputed from scratch in the same scheme adopted for the electroweak corrections. In Sec. V, we shall define the considered observables and show the results of our calculation, particular emphasis being given to the value of the total t-channel rate. A few conclusions will be drawn in Sec. VI.

II. THE t-CHANNEL PROCESSES AT ONE ELECTROWEAK LOOP

The complete description of the t channel involves at partonic level four subprocesses for single t production: $ub \to td$, $\bar{d}b \to t\bar{u}$, $cb \to ts$, $\bar{s}b \to t\bar{c}$, and the related four for the single $\bar{t}$ production. The starting point is the cross section for the $ub \to td$ process with the complete set of one-loop electroweak corrections (in the MSSM and SM). The $\mathcal{O}(\alpha)$ corrections to the (unpolarized) differential cross section of this process read

$$d\sigma^{\mathrm{ew}}_{ub\to td} = \frac{dt}{64\pi s^2}\sum_{\mathrm{spin}} 2\Re\mathrm{e}\{\mathcal{M}^{0*}\mathcal{M}^{1}\}, \tag{1}$$

where $\mathcal{M}^0$ is the tree level contribution to the amplitude of the partonic process $ub \to dt$ shown in Fig. 1, while $\mathcal{M}^1$ describes the electroweak one-loop contribution to the same amplitude. The Mandelstam variables are defined as

$$s = (p_b + p_u)^2 \qquad t = (p_b - p_t)^2 \qquad u = (p_b - p_d)^2. \tag{2}$$

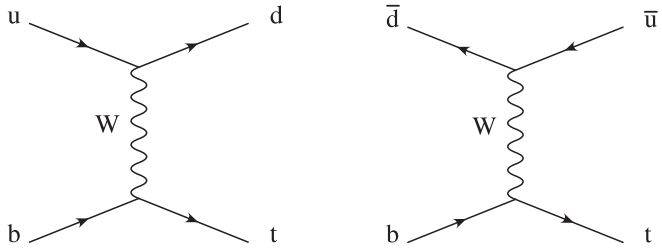

FIG. 1. Born direct and crossed processes for single top production in the t channel with first-generation light quark current.

The analytical expression for $\mathcal{M}^0$ is available in literature (see for instance [5]). $\mathcal{M}^1$ has been generated with the help of FEYNARTS [9], the algebraic reduction of the one-loop integrals is performed with the help of FORMCALC [10] and the scalar one-loop integrals are numerically evaluated using LOOPTOOLS [11]. We treat UV divergences using dimensional reduction while IR singularities are parametrized giving a small mass m_γ to the photon. The masses of the light quarks are used as regulators of the collinear singularities and are set to zero elsewhere.

UV divergences are cured renormalizing the parameters and the wavefunctions appearing in $\mathcal{M}^0$. In our case, we have to renormalize the wavefunction of the external quarks, the mass of the W boson, the Weinberg angle, and the electric charge. We use the on-shell scheme described in Ref. [12]. This scheme uses the fine structure constant evaluated in the Thompson limit as input parameter. In order to avoid large logarithms arising from the runnning of α to the electroweak scale M_W, we slightly modify this scheme using as input parameter the Fermi constant G_F. We consistently change the definition of the renormalization constant of the fine structure constant following the guidelines of Ref. [13].

The unpolarized differential cross section for the process $\bar{d}b \to \bar{u}t$ can be obtained from that of the process $ub \to td$ by crossing

$$d\sigma^{\mathrm{ew}}_{\bar{d}b\to\bar{u}t} = \frac{dt}{64\pi s^2}\sum_{\mathrm{spin}} 2\Re\mathrm{e}\{\mathcal{M}^{0*}(s \to u, u \to s) \times \mathcal{M}^{1}(s \to u, u \to s)\}. \tag{3}$$

For the $\bar{t}$ production the cross sections can be calculated using the identities

$$d\sigma^{\mathrm{ew}}_{ub\to td} = d\sigma^{\mathrm{ew}}_{\bar{u}\,\bar{b}\to\bar{d}\,\bar{t}} \qquad d\sigma^{\mathrm{ew}}_{\bar{d}b\to t\bar{u}} = d\sigma^{\mathrm{ew}}_{d\bar{b}\to u\bar{t}}, \tag{4}$$

while the processes involving the second-generation c, s and $\bar{s}$, $\bar{c}$ quarks can be computed from the previous, simply replacing the masses of the external particles (and some masses in the loop corrections).

III. QED EFFECTS

In order to obtain physically meaningful observables one has to include the differential cross section for the process of t-channel single top production associated with the emission of a photon integrated over the whole photonic phase space. So we have to consider the partonic processes $ub \to td\gamma$, $\bar{d}b \to t\bar{u}\gamma$, $cb \to ts\gamma$, $\bar{s}b \to t\bar{c}\gamma$, and the related four for the single $\bar{t}$ production. The unpolarized differential cross section of these processes has been obtained using two different procedures. In the first approach the amplitude has been generated and squared using FEYNARTS and FORMCALC , while in the second one the complete matrix element has been calculated with the help of FORM. The two methods are in mutual agreement. The phase-space integration of the aforementioned differential

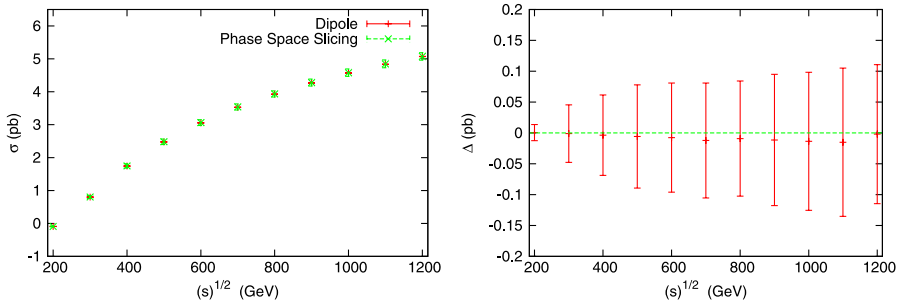

FIG. 2 (color online). Lowest-order partonic cross section for the process $ub \to dt\gamma$ computed with the two different methods. The cuts for the phase space slicing methods are $\delta_s = \delta_c = 10^{-4}$. The quantity Δ is defined as $\Delta = \sigma^{\text{Dipole}} - \sigma^{\text{Slicing}}$.

cross section is singular in the region in which the photon is soft and in the region in which it is collinear to a massless quark. According to the Kinoshita-Lee-Nauenberg theorem [14] IR singularities and the collinear singularities related to the final state radiation cancel in sufficiently inclusive observables, while the collinear singularities related to initial state radiation have to be absorbed in the redefinition of the parton distribution functions (PDF). In order to regularize these divergences we use two different procedures: the dipole subtraction method and the phase-space slicing method. In the subtraction approach one has to add and subtract to the squared amplitude an auxiliary function with the same asymptotic behavior and such that it can be analytically integrated over the photon phase space. Among the different choices we use the function quoted in Ref. [15]. In this reference, explicit expression for the subtraction function and for its analytical integration is obtained using the so-called dipole formalism [16]. The idea behind the phase-space slicing approach is to isolate the singular region of the phase space introducing a cutoff on the energy of the photon ($\Delta E = \delta_s \sqrt{s}/2$) and on the angle between the photon and the massless quarks (δ_c). In the regular region, the phase-space integration can be done numerically, while in the singular region it can be performed analytically provided that the cutoffs are small enough. The form of the differential cross section in the singular region is universal and its explicit expression in the soft (collinear) region can be found in Refs. [12,13]. As can be inferred from Fig. 2, the two methods are in good numerical agreement.

IV. ONE-LOOP SUSY QCD CORRECTIONS

The one-loop SUSY QCD corrections to t-channel single top production have been computed at LHC in Ref. [17]. We include these corrections recomputing them from scratch following the guidelines described in Sec. II. The only difference is that, following a standard procedure in SUSY QCD, we treat UV divergences using dimensional regularization. Moreover, in this case we have to renormalize only the wave functions of the squarks, since the other renormalization constant do not have $\mathcal{O}(\alpha_s)$ corrections. These corrections are IR safe.

V. OBSERVABLE QUANTITIES

The differential hadronic cross section reads

$$d\sigma(S) = \sum_{(q,q')} \int_{\tau_0}^{1} d\tau \frac{dL_{qb}}{d\tau} (d\sigma^{\text{ew}}_{qb\to q't}(s) + d\sigma^{\text{ew}}_{qb\to q't\gamma}(s) + d\sigma^{\text{SQCD}}_{qb\to q't}(s)) \frac{dL_{\bar{q}\,\bar{b}}}{d\tau} (d\sigma^{\text{ew}}_{\bar{q}\,\bar{b}\to\bar{q}'\bar{t}}(s) + d\sigma^{\text{ew}}_{\bar{q}\,\bar{b}\to\bar{q}'\bar{t}\gamma}(s) + d\sigma^{\text{SQCD}}_{\bar{q}\,\bar{b}\to\bar{q}'\bar{t}}(s)), \quad (5)$$

where $(q, q') = (u, d), (c, s), (\bar{d}, \bar{u}), (\bar{s}, \bar{d})$. The differential luminosity has been defined according to Ref. [18], while $\tau_0 = m_t^2/S$ and $s = \tau S$. $d\sigma^{\text{ew}}_X (d\sigma^{\text{SQCD}}_X)$ are the $\mathcal{O}(\alpha^3)$ (SUSY QCD) corrections to the differential cross section of the process X.

As pointed out in Sec. III, initial state collinear singularities are not cancelled in the sum of virtual and real corrections, and they are absorbed in the definition of the PDF. We use the $\overline{\text{MS}}$ factorization scheme at the scale $\mu_F = m_t$. Concerning the choice of the parton distributions set, we follow [13]. The calculation of the full $\mathcal{O}(\alpha)$ corrections to any hadronic observable must include QED effects in the Dokshitzer-Gribov-Lipatov-Altarelli-Parisi evolution equations. Such effects are taken into account in the MRST2004QED PDF [19], which are NLO QCD. Since our computation is leading-order QCD, we use the LO set CTEQ6L, since the QED effects are known to be small [20].

A. Numerical results

In this subsection, we present our numerical results. We define M_{inv} as the invariant mass of the (anti) top quark and of the light quark in the final state. Also, we denote by p_T the transverse momentum of the (anti) top quark. We consider as physical observables the transverse momentum distribution $\frac{d\sigma}{dp_T}$, the invariant mass distribution $\frac{d\sigma}{dM_{\text{inv}}}$, and two integrated observables derived from the previous: the integrated transverse momentum distribution, defined as the integral of $\frac{d\sigma}{dp_T}$ from a minimum p_T^{min} up to infinity

$$\sigma(p_T^{\min}) = \int_{p_T^{\min}}^{\infty} \frac{d\sigma}{dp_T'} dp_T' \tag{6}$$

and the cumulative invariant mass distribution $\sigma(M_{\rm inv}^{\max})$, defined as the integral of the invariant mass distribution from the production threshold up to $M_{\rm inv}^{\max}$

$$\sigma(M_{\rm inv}^{\max}) = \int_{\tau_0}^{M_{\rm inv}^{\max}} \frac{d\sigma}{dM_{\rm inv}'} dM_{\rm inv}'. \tag{7}$$

For each observable we present the plots for the LO and NLO curves and for the percentage effect of the NLO corrections to the observable ($\delta = \frac{\rm NLO-LO}{\rm NLO} \times 100$). Apart from the SM results, we analyzed several supersymmetric mSUGRA benchmark points: in the figures, we present the numerical results for the two representative ATLAS DC2 mSUGRA benchmark points SU1 and SU6 [21]; in the other cases, the results are similar. The SU1 and SU6 input parameters generate a moderately light supersymmetric scenarios, where the masses of the supersymmetric particles are below the 1 TeV: the two physical spectra are quite similar, characterized by relatively heavy squark sector (562–631 GeV for the lightest squark in SU1 and SU6, respectively), a light neutralino and a light chargino state. The typical masses for the supersymmetic Higgs are of order of 400–500 GeV. The main difference between the two points is the value of $\tan\beta$ input parameter: 10 for SU1 and 50 for SU6.

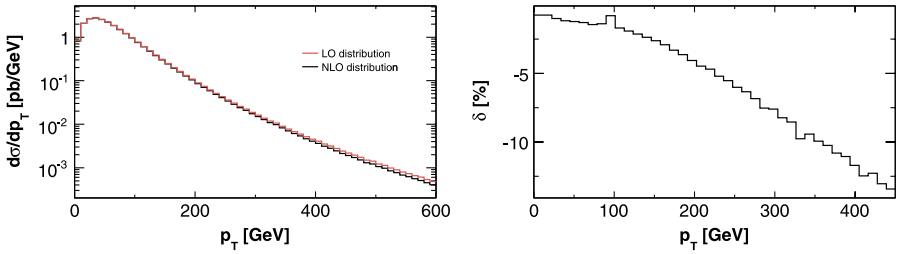

FIG. 3 (color online). Left panel: We plot the LO (that is tree level) contribution and the NLO; that is tree level plus $\mathcal{O}(\alpha^3)$corrections to the transverse momentum distribution. Right panel: We plot the percentage contribution of the $\mathcal{O}(\alpha^3)$ corrections to the transverse momentum distribution; that is $\delta = \frac{\rm NLO-LO}{\rm NLO} \times 100$. No cuts are imposed. Computation in the SM framework.

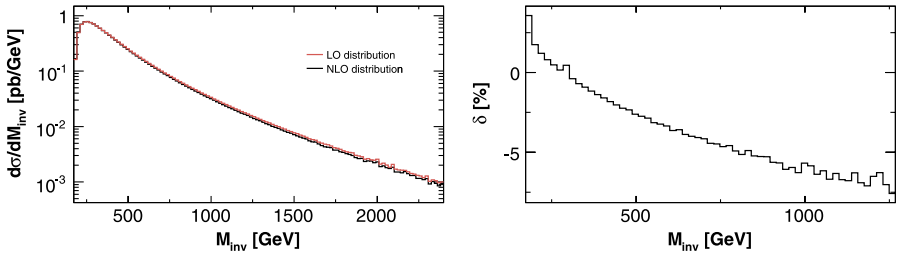

FIG. 4 (color online). Left panel: We plot the LO (that is tree level) contribution and the NLO; that is tree level plus $\mathcal{O}(\alpha^3)$ corrections to the invariant mass distribution. Right panel: We plot the percentage contribution of the $\mathcal{O}(\alpha^3)$ corrections to the invariant mass distribution; that is $\delta = \frac{\rm NLO-LO}{\rm NLO} \times 100$. No cuts are imposed. Computation in the SSM framework.

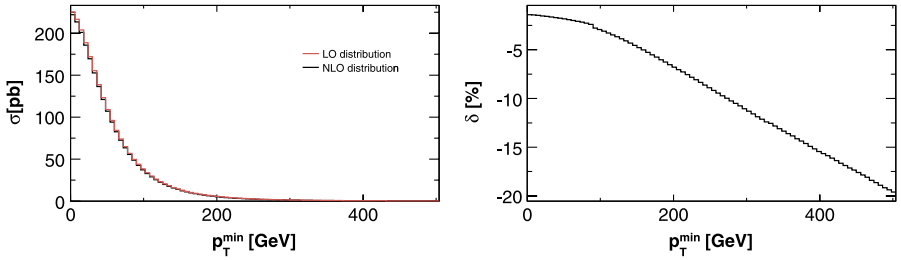

FIG. 5 (color online). Left panel: We plot the LO (that is tree level) contribution and the NLO; that is tree level plus $\mathcal{O}(\alpha^3)$ corrections to the integrated transverse momentum distribution $\sigma(p_T^{\min})$. We remind that this distribution is defined as the transverse momentum distribution integrated from a minimum $p_T^{\min}$ up to infinity. Right panel: We plot the percentage contribution of the $\mathcal{O}(\alpha^3)$ corrections to the integrated transverse momentum distribution; that is $\delta = \frac{\rm NLO-LO}{\rm NLO} \times 100$. No cuts are imposed. Computation in the SM framework.

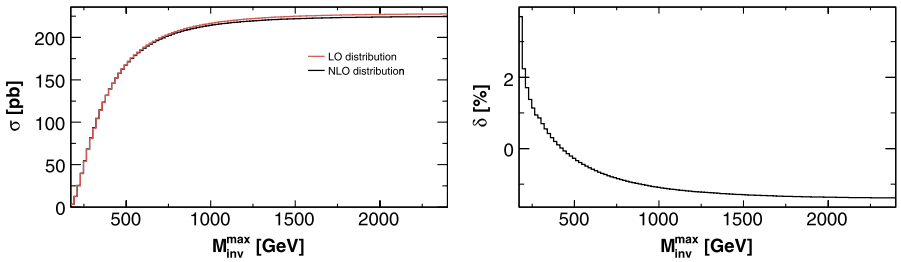

FIG. 6 (color online). Left panel: We plot the LO (that is tree level) contribution and the NLO; that is tree level plus $\mathcal{O}(\alpha^3)$ corrections to the cumulative invariant mass distribution $\sigma(M_{\rm inv}^{\rm max})$. We remind that this distribution is defined as the invariant mass distribution integrated from threshold up to $M_{\rm inv}^{\rm max}$. Right panel: We plot the percentage contribution of the $\mathcal{O}(\alpha^3)$ corrections to the cumulative invariant mass distribution; that is $\delta = \frac{\rm NLO-LO}{\rm NLO} \times 100$. No cuts are imposed. Computation in the SM framework.

1. SM results

In the SM framework the behavior of the four observables is shown in Figs. 3–6: the left panels report the LO and NLO curves, and the right panels show the relative percentage effect of the one-loop electroweak corrections: as one can see the curves for the NLO and LO are almost overlapping, and the global $\mathcal{O}(\alpha^3)$ NLO effect is rather small. This is particularly evident considering the plot for the cumulative invariant mass distribution, where the percentage effect saturate to the $\simeq 1.5\%$ for $M_{\rm inv} > 1500$ GeV.

2. MSSM results

The following figures show the analogous results for the transverse momentum distribution $\frac{d\sigma}{dp_T}$, the invariant mass distribution $\frac{d\sigma}{dM_{\rm inv}}$, the integrated p_T ditribution $\sigma(p_T^{\rm min})$, and the cumulative invariant mass distribution 7–10) and for the SU6 (Figs. 11–14) benchmark points. In the MSSM cases, the NLO is defined as the sum of the electroweak part $\mathcal{O}(\alpha^3)$ and of the SUSY QCD part; in each figure, we show in the panel (a) the behavior of the observable at LO and NLO; in (b) the global NLO effect (where "global" means $\mathcal{O}(\alpha^3)$ plus SUSY QCD); in (c) and (d) the separate percentage contributions of the $\mathcal{O}(\alpha^3)$ and SUSY QCD parts, respectively.

A first comment that can be drawn from the inspection of the plots is that the t-channel process is very weakly sensitive to the presence of the supersymmetric particle in the loops. The difference with the SM case, below the percent level, is negligible for both the mSUGRA bench-

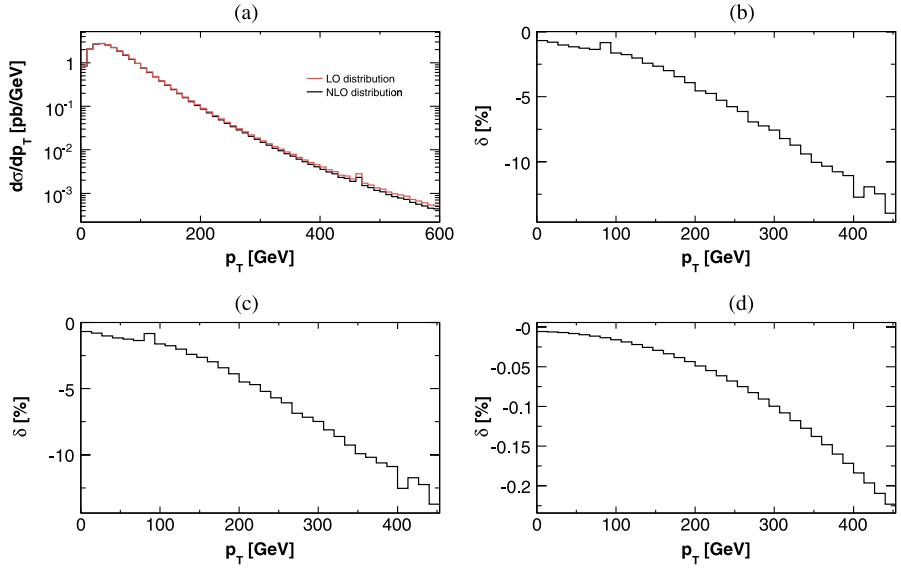

FIG. 7 (color online). (a) We plot the LO (that is tree level) contribution and the NLO; that is tree level plus $\mathcal{O}(\alpha^3)$ plus SUSY QCD corrections to the transverse momentum distribution. (b) We plot the percentage contribution of the $\mathcal{O}(\alpha^3)$ plus SUSY QCD corrections to the transverse momentum distribution; that is $\delta = \frac{\rm NLO-LO}{\rm NLO} \times 100$. (c) We plot the percentage contribution of the $\mathcal{O}(\alpha^3)$ corrections to the transverse momentum distribution; that is $\delta = \frac{\mathcal{O}(\alpha^3)}{\rm NLO} \times 100$. (d) We plot the percentage contribution of the SUSY QCD corrections to the transverse momentum distribution; that is $\delta = \frac{\rm SUSY\ QCD}{\rm NLO} \times 100$. No cuts are imposed. Computation in the SU1 point.

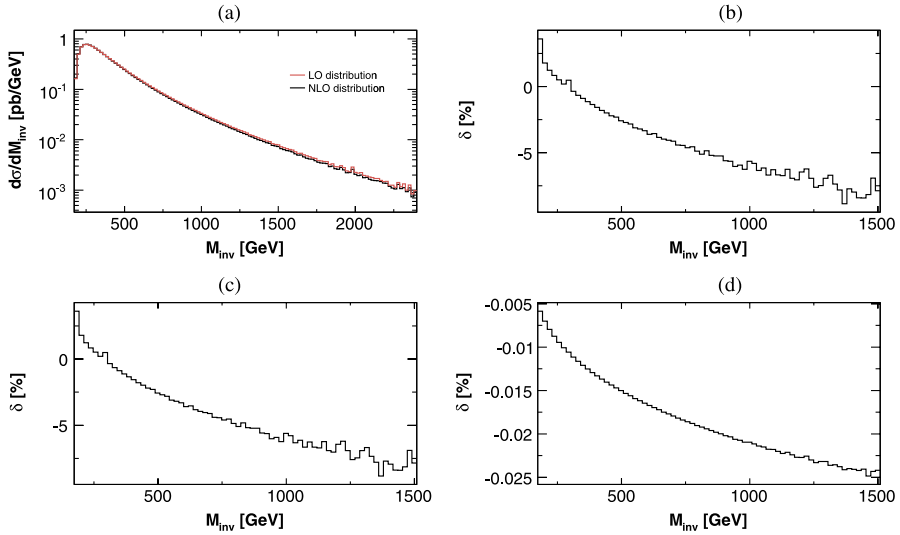

FIG. 8 (color online). (a) We plot the LO (that is tree level) contribution and the NLO; that is tree level plus $\mathcal{O}(\alpha^3)$ plus SUSY QCD corrections to the invariant mass distribution. (b) We plot the percentage contribution of the $\mathcal{O}(\alpha^3)$ plus SUSY QCD corrections to the invariant mass distribution; that is $\delta = \frac{\text{NLO}-\text{LO}}{\text{NLO}} \times 100$. (c) We plot the percentage contribution of the $\mathcal{O}(\alpha^3)$ corrections to the invariant mass distribution; that is $\delta = \frac{\mathcal{O}(\alpha^3)}{\text{NLO}} \times 100$. (d) We plot the percentage contribution of the SUSY QCD corrections to the invariant mass distribution; that is $\delta = \frac{\text{SUSY QCD}}{\text{NLO}} \times 100$. No cuts are imposed. Computation in the SU1 point.

mark points, without appreciable differences between the two sets. The plots for percentage effect of the SUSY QCD corrections only (the (d) panel in Figs. 7–10 for SU1 and 11–14 for SU6) show that the contribution of diagrams with virtual squark and gluinos is systematically small, below the 1% level, in agreement with Ref. [17]. The same conclusion holds for the pure electroweak supersymmetric contribution, being the $\mathcal{O}(\alpha^3)$ effect due almost completely to the SM part.

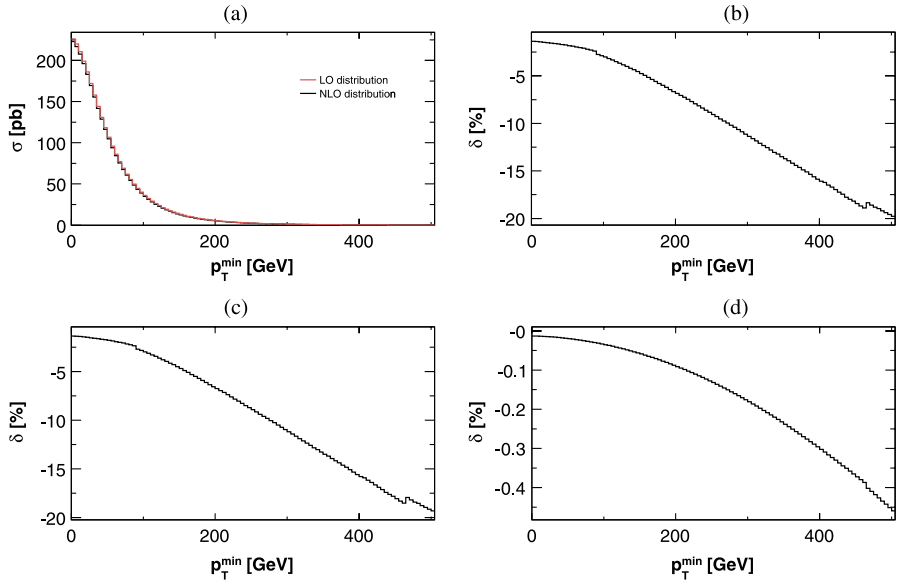

FIG. 9 (color online). (a) We plot the LO (that is tree level) contribution and the NLO; that is tree level plus $\mathcal{O}(\alpha^3)$ plus SUSY QCD corrections to the integrated transverse momentum distribution $\sigma(p_T^{\min})$. (b) We plot the percentage contribution of the $\mathcal{O}(\alpha^3)$ plus SUSY QCD corrections to the integrated transverse momentum distribution; that is $\delta = \frac{\text{NLO}-\text{LO}}{\text{NLO}} \times 100$. (c) We plot the percentage contribution of the $\mathcal{O}(\alpha^3)$ corrections to the integrated transverse momentum distribution; that is $\delta = \frac{\mathcal{O}(\alpha^3)}{\text{NLO}} \times 100$. (d) We plot the percentage contribution of the SUSY QCD corrections to the integrated transverse momentum distribution; that is $\delta = \frac{\text{SUSY QCD}}{\text{NLO}} \times 100$. No cuts are imposed. Computation in the SU1 point.

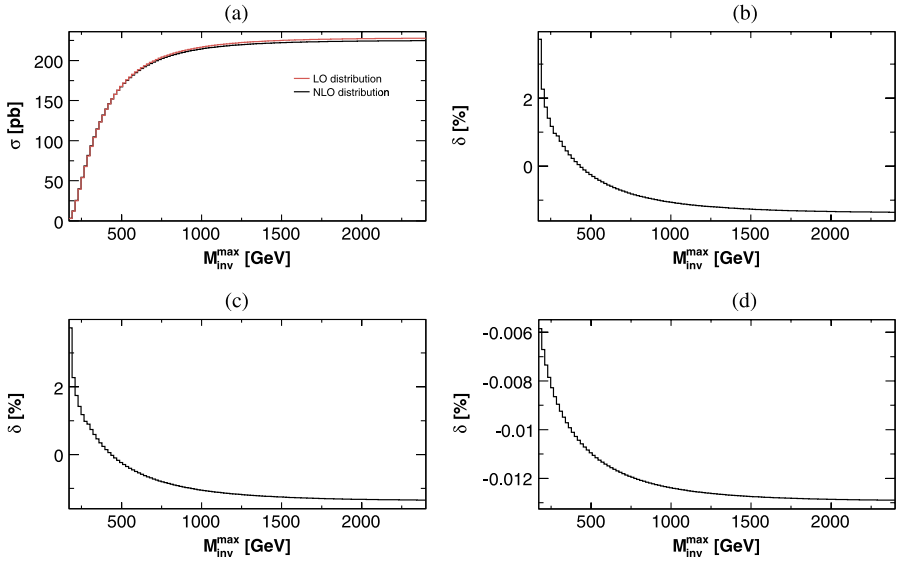

FIG. 10 (color online). (a) We plot the LO (that is tree level) contribution and the NLO; that is tree level plus $\mathcal{O}(\alpha^3)$ plus SUSY QCD corrections to the cumulative invariant mass distribution $\sigma(M_{\mathrm{inv}}^{\max})$. (b) We plot the percentage contribution of the $\mathcal{O}(\alpha^3)$ plus SUSY QCD corrections to the cumulative invariant mass distribution; that is $\delta = \frac{\mathrm{NLO-LO}}{\mathrm{NLO}} \times 100$. (c) We plot the percentage contribution of the $\mathcal{O}(\alpha^3)$ corrections to the cumulative invariant mass distribution; that is $\delta = \frac{\mathcal{O}(\alpha^3)}{\mathrm{NLO}} \times 100$. (d) We plot the percentage contribution of the SUSY QCD corrections to the cumulative invariant mass distribution; that is $\delta = \frac{\mathrm{SUSY\ QCD}}{\mathrm{NLO}} \times 100$. No cuts are imposed. Computation in the SU1 point.

3. PDF uncertainties

An important source of theoretical uncertainty is given by the contribution of the parametric errors associated with the parton densities. This could become particularly relevant for single top channels, due to the presence of an initial state b quark, whose distribution function is strictly related to the gluon distribution. We have studied the impact of such uncertainties on the transverse momentum

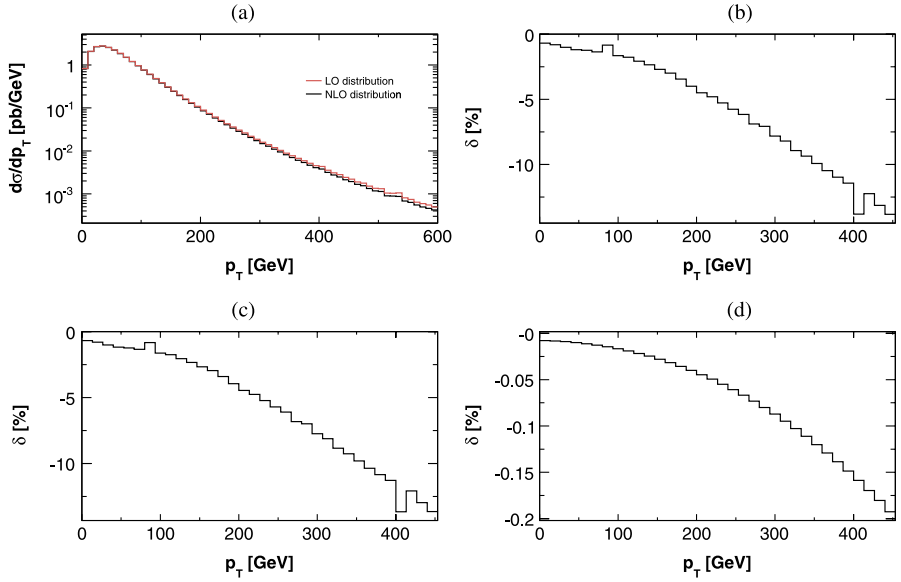

FIG. 11 (color online). (a) We plot the LO (that is tree level) contribution and the NLO; that is tree level plus $\mathcal{O}(\alpha^3)$ plus SUSY QCD corrections to the transverse momentum distribution. (b) We plot the percentage contribution of the $\mathcal{O}(\alpha^3)$ plus SUSY QCD corrections to the transverse momentum distribution; that is $\delta = \frac{\mathrm{NLO-LO}}{\mathrm{NLO}} \times 100$. (c) We plot the percentage contribution of the $\mathcal{O}(\alpha^3)$ corrections to the transverse momentum distribution; that is $\delta = \frac{\mathcal{O}(\alpha^3)}{\mathrm{NLO}} \times 100$. (d) We plot the percentage contribution of the SUSY QCD corrections to the transverse momentum distribution; that is $\delta = \frac{\mathrm{SUSY\ QCD}}{\mathrm{NLO}} \times 100$. No cuts are imposed. Computation in the SU6 point.

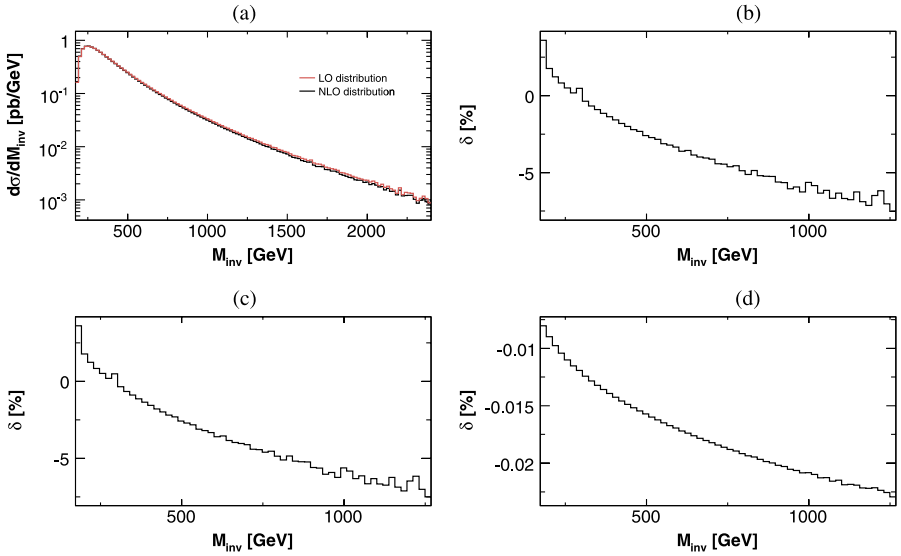

FIG. 12 (color online). (a) We plot the LO (that is tree level) contribution and the NLO; that is tree level plus $\mathcal{O}(\alpha^3)$ plus SUSY QCD corrections to the invariant mass distribution. (b) We plot the percentage contribution of the $\mathcal{O}(\alpha^3)$ plus SUSY QCD corrections to the invariant mass distribution; that is $\delta = \frac{\text{NLO}-\text{LO}}{\text{NLO}} \times 100$. (c) We plot the percentage contribution of the $\mathcal{O}(\alpha^3)$ corrections to the invariant mass distribution; that is $\delta = \frac{\mathcal{O}(\alpha^3)}{\text{NLO}} \times 100$. (d) We plot the percentage contribution of the SUSY QCD corrections to the invariant mass distribution; that is $\delta = \frac{\text{SUSY QCD}}{\text{NLO}} \times 100$. No cuts are imposed. Computation in the SU6 point.

distribution $\frac{d\sigma}{dp_T}$ and on the invariant mass distribution $\frac{d\sigma}{dM_{\text{inv}}}$ by using the PDF sets MRST2001E and CTEQ61E as in the LHAPDF package [22]. For each bin in the histograms the maximum and minimum values are calculated starting from the central value according to the formula $\sigma\,(\text{central}) \pm 1/2\sqrt{\sum_{i=20(15)}(\sigma(2i-1)-\sigma(2i))^2}$, according to the prescription of Ref. [23]. The results are shown in Fig. 15. The spread of the predictions obtained with the MRST set, displays a relative deviation of about 2% or less, increasing on the large-scale tails of the dis-

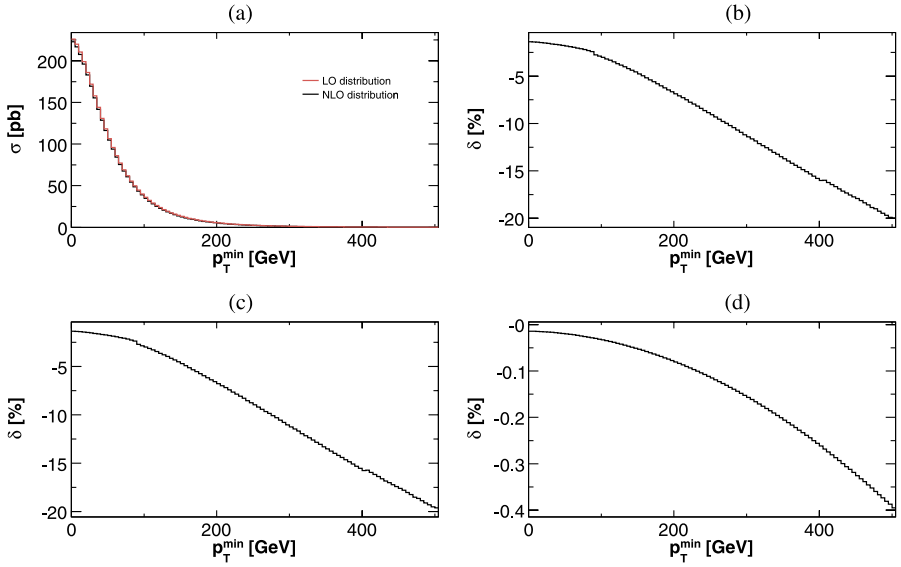

FIG. 13 (color online). (a) We plot the LO (that is tree level) contribution and the NLO; that is tree level plus $\mathcal{O}(\alpha^3)$ plus SUSY QCD corrections to the integrated transverse momentum distribution $\sigma(p_T^{\text{min}})$. (b) We plot the percentage contribution of the $\mathcal{O}(\alpha^3)$ plus SUSY QCD corrections to the integrated transverse momentum distribution; that is $\delta = \frac{\text{NLO}-\text{LO}}{\text{NLO}} \times 100$. (c) We plot the percentage contribution of the $\mathcal{O}(\alpha^3)$ corrections to the integrated transverse momentum distribution; that is $\delta = \frac{\mathcal{O}(\alpha^3)}{\text{NLO}} \times 100$. (d) We plot the percentage contribution of the SUSY QCD corrections to the integrated transverse momentum distribution; that is $\delta = \frac{\text{SUSY QCD}}{\text{NLO}} \times 100$. No cuts are imposed. Computation in the SU6 point.

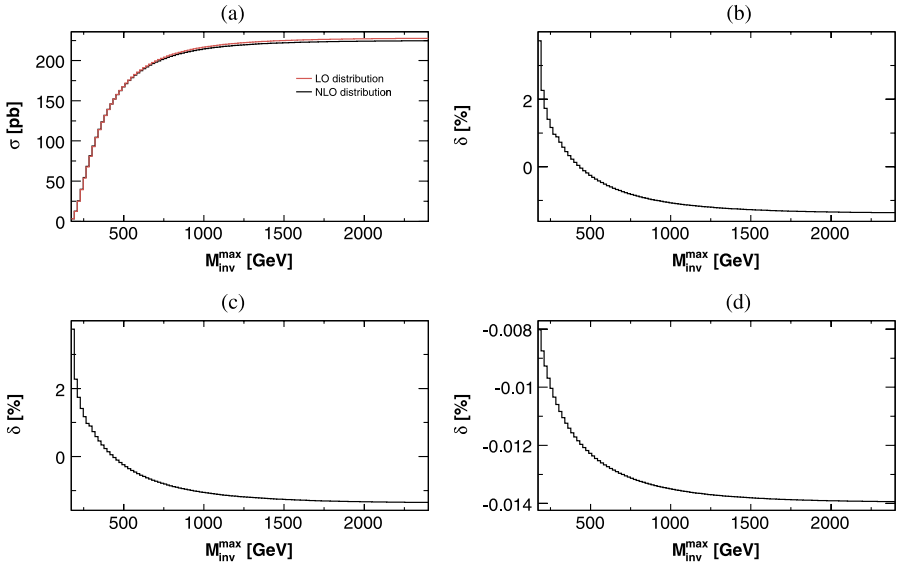

FIG. 14 (color online). (a) We plot the LO (that is tree level) contribution and the NLO; that is tree level plus $\mathcal{O}(\alpha^3)$ plus SUSY QCD corrections to the cumulative invariant mass distribution $\sigma(M_{\rm inv}^{\rm max})$. (b) We plot the percentage contribution of the $\mathcal{O}(\alpha^3)$ plus SUSY QCD corrections to the cumulative invariant mass distribution; that is $\delta = \frac{\rm NLO-LO}{\rm NLO} \times 100$. (c) We plot the percentage contribution of the $\mathcal{O}(\alpha^3)$ corrections to the cumulative invariant mass distribution; that is $\delta = \frac{\mathcal{O}(\alpha^3)}{\rm NLO} \times 100$. (d) We plot the percentage contribution of the SUSY QCD corrections to the cumulative invariant mass distribution; that is $\delta = \frac{\rm SUSY\ QCD}{\rm NLO} \times 100$. No cuts are imposed. Computation in the SU6 point.

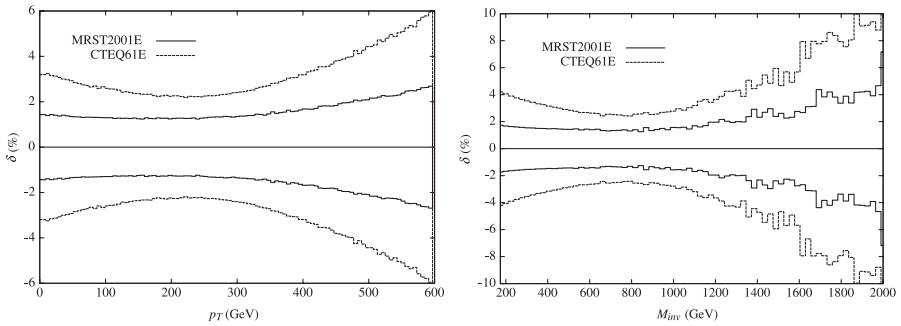

FIG. 15. Left panel: PDF uncertainty (in percent) on the $\frac{d\sigma}{dp_T}$ distribution (LO calculation). For each bin, the minimum and maximum deviations with respect to the best fit PDF, as given by the MRST2001E set (solid lines) and by the CTEQ61E set (dashed lines), are shown. Right: the same as in the left panel, for $\frac{d\sigma}{dM_{\rm inv}}$.

tributions (where the cross section is however very small), while the CTEQ set gives a larger uncertainty, of the order of 3–4%. This is due to different values of the tolerance parameter [24], the latter being defined as the allowed maximum of the $\Delta\chi^2$ variation with respect to the parameters of the best PDFs fit. Conservatively, we can associate to our predictions an uncertainty due to the present knowledge of parton densities of about 3%. It is also worth noting that the uncertainties obtained according to such a procedure are of purely experimental origin only (i.e. as due to the systematic and statistical errors of the data used in the global fit), leaving aside other sources of uncertainty of theoretical origin.

VI. CONCLUSIONS

We have computed in this paper the complete one-loop electroweak effect on various observables in the MSSM. The calculation has fully included QED effects. The overall result is that the one-loop effect is small, of a positive few percent in the total rate that we have considered as the first realistically measurable quantity. Technically speaking, this small number arises from a competition of negative weak contributions and positive QED terms. In the considered mSUGRA symmetry breaking scheme, the genuine SUSY effect in the considered benchmark points is systematically modest, at most of a 1% size. The values

that we have obtained, e.g. for the total rate should still be modified by the additional NLO QCD contribution. The latter is known, small and theoretically safe and could be easily added to our calculation. It will appear in a forthcoming paper that will provide an expression for the overall single top production at LHC, including the already existing calculations for the associated tW production (our paper and the QCD ones). We have also given an estimate of the parametric errors associated with the present knowledge of the parton densities. The distributions studied in this paper are affected by a few percent PDF uncertainty. It is worth saying that this uncertainty is expected to be lowered once the LHC data become available. In conclusion, a precise measurement of the t-channel rate appears as a perfect way to determine the value of the V_{tb} coupling, both within the SM and within the MSSM with mSUGRA symmetry breaking. We cannot exclude, though, that for different symmetry breaking mechanisms the genuine SUSY effect is more sizable. This question, which is beyond the purposes of this preliminary paper, remains open and, in our opinion, would deserve a special dedicated rigorous analysis.

ACKNOWLEDGMENTS

We are gratefull to T. Hahn and S. Pozzorini for helpful discussions. E. M. is indebted with S. Dittmaier for valuable suggestions on the dipole subtraction formalism.

[1] T. M. P. Tait, Phys. Rev. D **61**, 034001 (1999).
[2] J. Alwall *et al.*, Eur. Phys. J. C **49**, 791 (2007).
[3] J. Pumplin, D. R. Stump, J. Huston, H. L. Lai, P. Nadolsky, and W. K. Tung, J. High Energy Phys. 07 (2002) 012.
[4] T. Stelzer, Z. Sullivan, and S. Willenbrock, Phys. Rev. D **56**, 5919 (1997).
[5] M. Beccaria, G. Macorini, F. M. Renard, and C. Verzegnassi, Phys. Rev. D **74**, 013008 (2006).
[6] B. W. Harris, E. Laenen, L. Phaf, Z. Sullivan, and S. Weinzierl, Phys. Rev. D **66**, 054024 (2002); Z. Sullivan, Phys. Rev. D **70**, 114012 (2004); **72**, 094034 (2005); S. Zhu, Phys. Lett. B **524**, 283 (2002); **537**, 351(E) (2002); E. E. Boos, V. E. Bunichev, L. V. Dudko, V. I. Savrin, and A. V. Sherstnev, Phys. At. Nucl. **69**, 1317 (2006).
[7] J. Campbell, R. K. Ellis, and F. Tramontano, Phys. Rev. D **70**, 094012 (2004); Q.-H. Cao and C. P. Yuan, Phys. Rev. D **71**, 054022 (2005); Q.-H. Cao, R. Schwienhorst, and C. P. Yuan, Phys. Rev. D **71**, 054023 (2005); Q.-H. Cao, R. Schwienhorst, J. A. Benitez, R. Brock, and C. P. Yuan, Phys. Rev. D **72**, 094027 (2005); J. Campbell and F. Tramontano, Nucl. Phys. **B726**, 109 (2005).
[8] S. Frixione, E. Laenen, P. Motylinski, and B. R. Webber, J. High Energy Phys. 03 (2006) 092; S. Frixione, AIP Conf. Proc. **792**, 685 (2005).
[9] T. Hahn, Comput. Phys. Commun. **140**, 418 (2001); T. Hahn and C. Schappacher, Comput. Phys. Commun. **143**, 54 (2002).
[10] T. Hahn and M. Perez-Victoria, Comput. Phys. Commun. **118**, 153 (1999).
[11] T. Hahn, Acta Phys. Pol. B **30**, 3469 (1999); T. Hahn, Nucl. Phys. B, Proc. Suppl. **89**, 231 (2000); T. Hahn and M. Rauch, Nucl. Phys. B, Proc. Suppl. **157**, 236 (2006).
[12] A. Denner, Fortschr. Phys. **41**, 307 (1993).
[13] J. H. Kuhn, A. Kulesza, S. Pozzorini, and M. Schulze, Nucl. Phys. **B797**, 27 (2008); W. Hollik, T. Kasprzik, and B. A. Kniehl, Nucl. Phys.**B790**, 138 (2008).
[14] T. Kinoshita, J. Math. Phys. (N.Y.) **3**, 650 (1962); T. D. Lee and M. Nauenberg, Phys. Rev. B **133**, B1549 (1964).
[15] S. Dittmaier, Nucl. Phys. **B565**, 69 (2000).
[16] S. Catani and M. H. Seymour, Phys. Lett. B **378**, 287 (1996); Nucl. Phys. **B485**, 291 (1997).**B510**, 503 (1998); S. Catani, S. Dittmaier, M. H. Seymour, and Z. Trocsanyi, Nucl. Phys. **B627**, 189 (2002).
[17] J. J. Zhang, C. S. Li, Z. Li, and L. L. Yang, Phys. Rev. D **75**, 014020 (2007).
[18] R. K. Ellis, W. J. Stirling, and B. R. Webber, Cambridge Monogr. Part. Phys., Nucl. Phys., Cosmol. **8**, 1 (1996).
[19] A. D. Martin, R. G. Roberts, W. J. Stirling, and R. S. Thorne, Eur. Phys. J. C **39**, 155 (2005).
[20] M. Roth and S. Weinzierl, Phys. Lett. B **590**, 190 (2004).
[21] ATLAS Data Challenge 2 DC2 points; http://paige.home.cern.ch/paige/fullsusy/romeindex.html.
[22] http://hepforge.cedar.ac.uk/lhapdf/; M. R. Whalley, D. Bourilkov, and R. C. Group, arXiv:hep-ph/0508110, and references therein.
[23] http://durpdg.dur.ac.uk/hepdata/pdf3.html.
[24] A. D. Martin, R. G. Roberts, W. J. Stirling, and R. S. Thorne, Eur. Phys. J. C **28**, 455 (2003); J. Pumplin, D. R. Stump, J. Houston, H. L. Lai, P. Nadolsky, and W. K. Tung, J. High Energy Phys. 07 (2002) 012.